Electronic Supplementary Material (ESI) for RSC Advances.

This journal is © The Royal Society of Chemistry 2020

Supplementary Material (ESI) for RSC Advances

This journal is (c) The Royal Society of Chemistry 2020

Electronic Supplementary Information

The influence of the titania morphology and hydroxyapatite on the proliferation and osteogenic differentiation of human mesenchymal stem cells

Yauheni U. Kuvyrkou[a, b], Nadzeya Brezhneva[c], Ekaterina V. Skorb[d], Sviatlana A. Ulasevich*[d]

[a]Republican Scientific and Practical Center of Transfusiology and Medical Biotechnologies, Dolginovskiy tract 160, 220053 Minsk, Belarus

[b]Belarusian State Technological University, Sverdlova str. 13a, 220006 Minsk, Belarus

[c]Chemistry Department, Belarusian State University, Leningradskaya str. 14, 220030 Minsk, Belarus

[d]ITMO University, Lomonosova str. 9, 191002 St. Petersburg, Russia. E-mail: saulasevich@itmo.ru

Corresponding author. E-mail: saulasevich@itmo.ru

We have chosen the titanium dioxide nanotubes modified by hydroxyapatite (TNT-HA) as the most convenient system to compare the energy dispersive X-ray spectrometer (EDS) method and the Glow Discharge Optical Emission Spectroscopy (GDOES). The energy-dispersive X-ray spectroscopy (EDS) was done using Hitachi SU-70 microscopes coupled with a Bruker EDS detector at an operating voltage of 15 kV. The GDOES method allows to estimate the coating composition profile across the formed layer. In GDOES, the samples act as one of the electrodes of the plasma and are supposed to close the plasma chamber[1–3]. The samples were mounted with copper tape to cover the anode. The anode diameter was of 4 mm. Analyses were performed in a nitrogen atmosphere at a pressure of 650 Pa and at a constant power of 30 W. The depth profile was made via the continuous process of sputtering through a sample at the rate of 3 μm. The depth and layer thickness were calculated relying on the use of profilometers to accurately provide the mandatory depth information. As can be seen from Fig. S1b, the content of calcium and phosphorus near the surface region is higher than inside of the nanotubes. The EDS profile of TNT-HA shows a similar tendency. Thus, we can use these two methods for analysis the depth profile.

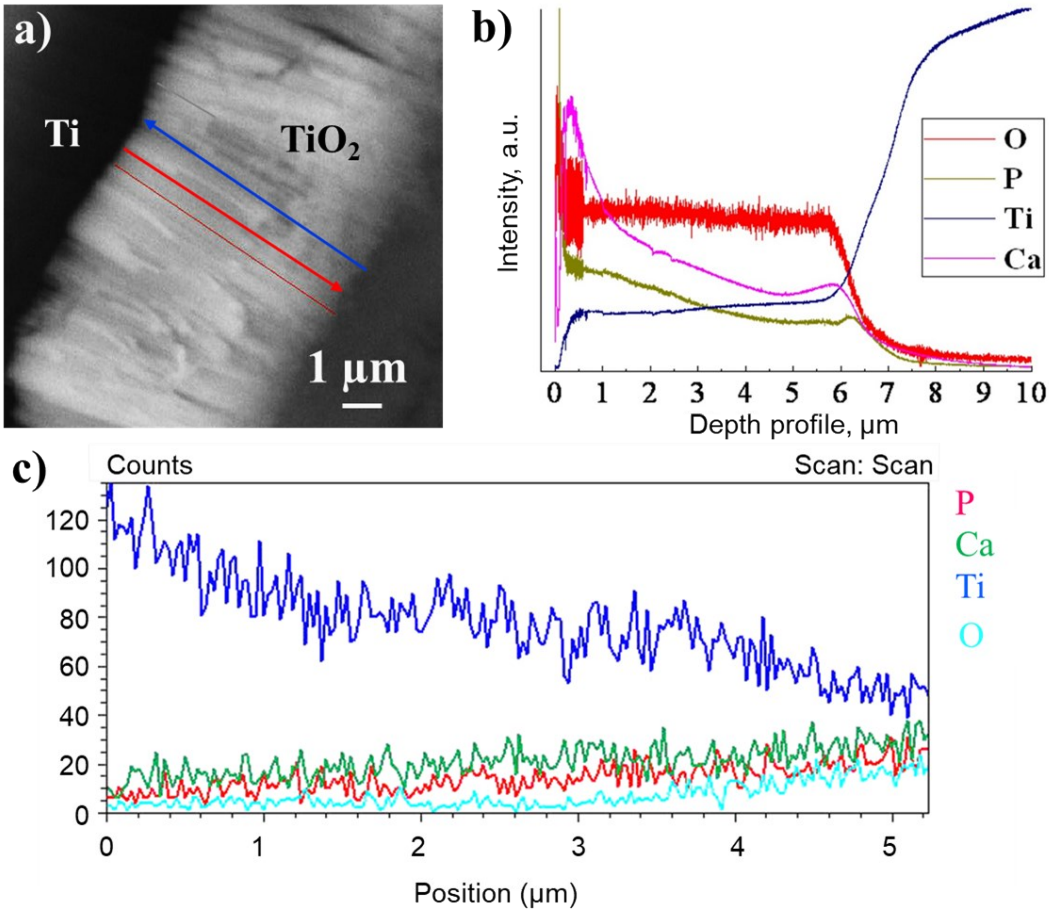

Fig. S1. a) SEM image (cross-section) of titania nanotubes modified by hydroxyapatite (TNT-HA); b) The GDOES depth profile of TNT-HA. The profile was measured along the blue arrow; c) EDS profile of TNT-HA. The profile was measured along the red arrow.

The osteogenic differentiation of hMSCs have been analysed by a reverse transcription-quantitative polymerase chain reaction in real-time (RT-qPCR). The expression of the osteocalcin gene, a specific marker for the osteogenic differentiation of stem cells, and the alkaline phosphatase gene is determined by RT-qPCR.

After 14 days of culture, the cells were lysed and total RNA was isolated by TRI-reagent. The RNA samples were treated with DNAse and reverse-transcribed using Revertaid Reverse Transcriptase according to the program: 25°C for 10 min, 50°C for 30 min, 85°C for 5 min. The RT-qPCR allows comparing gene expression quantitatively. The RT-qPCR was carried out using a thermocycler for analysing the expression of runt-related transcription factor 2 (RUNX2), C-MYC, alkaline phosphatase (ALP), collagen type

I (COL I), osteocalcin (OCN), osteopontin (OSP), protein tyrosine kinase 2 (PTK2), extracellular signal-regulated kinase 1/2 (ERK 1/2), cell-cycle-related transcription factor (E2F1), retinoblastoma-associated protein (RB), cyclin-dependent kinase 6 (CDK6), cyclin D1, glyceraldehyde 3-phosphate dehydrogenase (GAPDH) genes. Primer sequences and amplicon sizes produced by PrimeTech (Belarus) for these genes were following: ALP forward primer 5'-ACAACTACCAGGCGCAGTCT-3', ALP reverse primer 5'-CAGAACAGGACGCTCAGG-3', 260 bp; COL I forward primer 5'-TGCTCGTGGAAATGATGGTG-3', COL I reverse primer 5'-CTTCACCCTTAGCACCAACAG-3', 104 bp; OSC forward primer 5'-GCCCTCACACTCCTCGCC-3', OSC reverse primer5'-CTACCTCGCTGCCCTCCTG-3', 130 bp; OSP forward primer 5'-ACAGCCGTGGGAAGGACAGT-3', OSP reverse primer 5'-GACTGCTTGTGGCTGTGGGT-3', 76 bp; RUNX 2 forward primer 5'-CAGACCAGCAGCACTCCATA-3', RUNX 2 reverse primer CAGCGTCAACACCATCATTC-3', 178 bp; C-MYC forward primer 5'-TTTCTACTGCGACGAGGAGG-3', C-MYC reverse primer 5'-GGCAGCAGCTCGAATTTCTT-3', 105 bp; PTK 2 forward primer 5'-GTCTGCCTTCGCTTCACG-3', PTK 2 reverse primer 5'- GCCGAGATCATGCCACTC-3', 92 bp; ERK 1 forward primer 5'-CCCTAGCCCAGACAGACATC-3', ERK 1 reverse primer 5'- GCACAGTGTCCATTTTCTAACAGT-3', 94 bp; ERK 2 forward primer 5'-TCTGCACCGTGACCTCAA-3', ERK 2 reverse primer 5'- GCCAGGCCAAAGTCACAG-3', 78 bp; E2F1 forward primer 5'-CACTTTCGGCCCTTTTGCTC-3', E2F1 reverse primer 5'-GATTCCCCAGGCTCACCAAA-3', 212 bp; RB forward primer 5'-TTTGTAACGGGAGTCGGGAG-3', RB reverse primer 5'- ATCGAACTGCTGGGTTGTGT-3', 648 bp; CDK6 forward primer 5'-CGGAGAGAGTGCTGGTAACTC-3', CDK6 reverse primer 5'-CCTCGAAGCGAAGTCCTCAA-3', 204 bp; cyclin D1 forward primer 5'-ACACGGACTACAGGGGAGTTT-3', cyclin D1 reverse primer 5'-GGAAGCGGTCCAGGTAGTTC-3', 473 bp; GAPDH forward primer 5'-TCAAGGCTGAGAACGGGAA-3', GAPDH reverse primer 5'-TGGGTGGCAGTGATGGCA-3', 376 bp. GAPDH served as a house-keeping gene, and the expression of the genes of interest was normalized to GAPDH expression. For the quantification of gene expression, $2^{-\Delta\Delta CT}$-method was used[4-5]. The relative transcript level was represented as mean ± 95% confidence interval (n = 3 for each group) for plotting the graphs. Statistical analysis was carried out using GraphPad Software.

In general, differentiation is a process of turning undifferentiated cells into specialized cells of tissue or blood. It is a difficult multistage process. At the various stages of differentiation, cells are characterized by various markers. Osteocalcin (OSC) is a specific marker for the osteogenic differentiation of stem cells. Osteocalcin, produced by osteoblasts, is only in bone tissue and dentine[6-8]. Cells don't produce inorganic substances. Indirectly, alkaline phosphatase can be used for the evidence of extracellular mineralization. Alkaline phosphatase hydrolyzes the phosphate esters and takes a central part in skeletal mineralization[9,10].

In this paper, we demonstrate the expression of the osteocalcin gene and alkaline phosphatase gene by RT-qPCR to prove the osteogenic differentiation of stem cells.
Human AB group serum was previously reported to maintain the differentiation of hMSCs into the osteogenic direction[9,10]. Collagen type I is the most abundant protein in bone tissue[11]. It forms more than 90 % of the organic part of bone tissue37. Alkaline phosphatase hydrolyzes the phosphate esters and takes a central part in skeletal mineralization38. A lot of alkaline phosphatase is located in bone tissue and this enzyme hydrolyzes the phosphate esters and takes a central part in skeletal mineralization[11]. Osteocalcin is systematically utilized as a marker for the advent of osteogenic commitment as it is manifested by osteoblasts after the proliferation[9]. Collagen type I is the most abundant protein in bone tissue36. It forms more than 90 % of the organic part of bone tissue[12]. Alkaline phosphatase hydrolyzes the phosphate esters and takes a central part in skeletal mineralization[13]. A lot of alkaline phosphatase is located in bone tissue and this enzyme provides the mineralization exchange[14]. Cells do not produce inorganic substances. Consequently, alkaline phosphate can indirectly be used for the detection of extracellular mineralization. Osteocalcin is systematically utilized as a marker for the advent of osteogenic commitment as it is manifested by osteoblasts after the

proliferation[14]. Osteocalcin is found in bone tissue and dentine[14-15]. Thus, osteocalcin is a unique marker for the osteogenic differentiation of stem cells. Osteopontin is a calcium binding non-collagenous protein of bone tissue which contains the tripeptide sequence of arginine, glycine, aspartic acid (RGD) facilitating the focal adhesion of cells via integrin attaching[15-16].

Here, we demonstrate the expression of these genes by RT-qPCR to prove the osteogenic differentiation of hMSCs (Fig. S2).

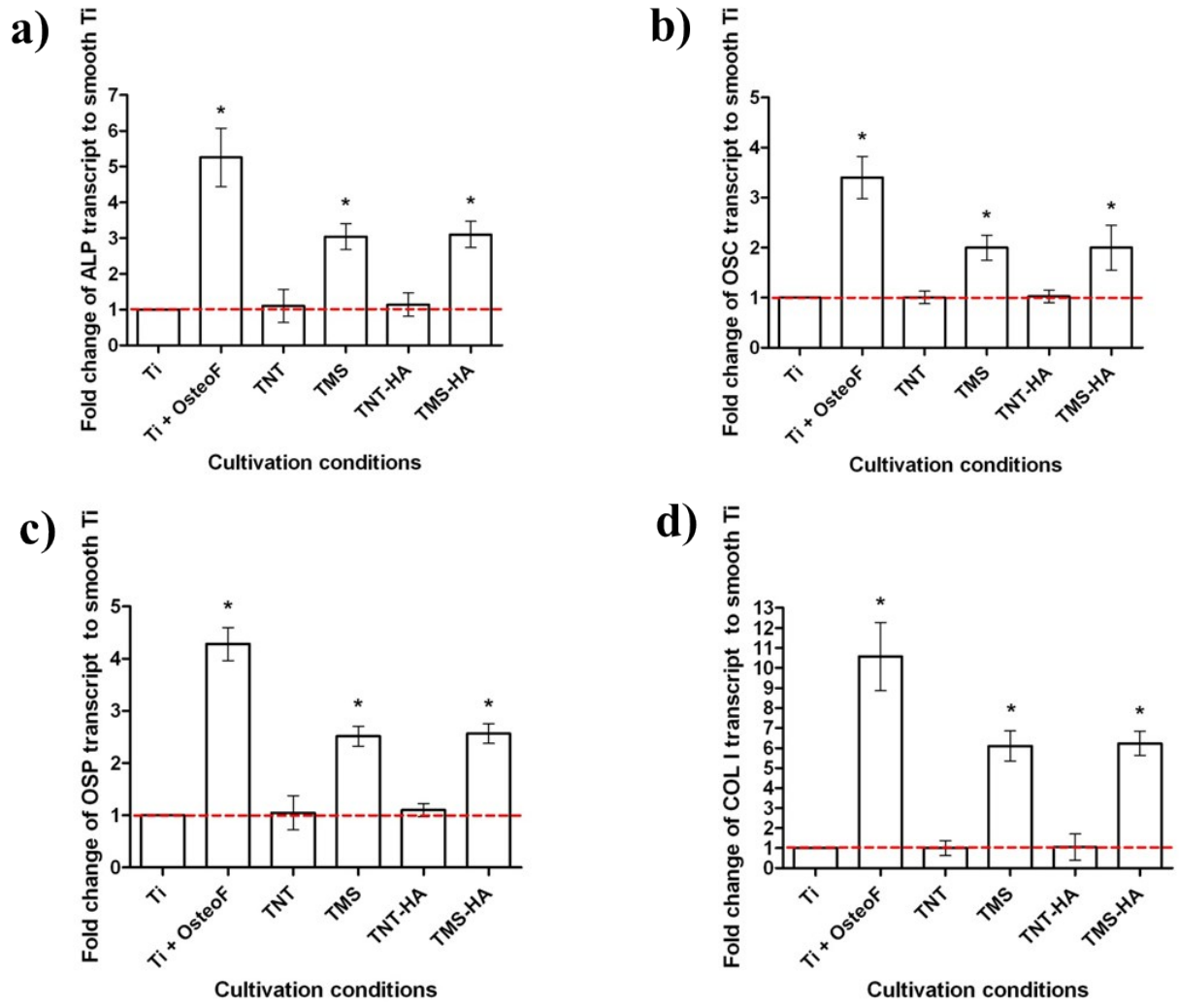

Fig. S2. Expression of critical osteoblast genes after 14-day incubation of mesenchymal stem cells on interfaces. (a) - alkaline phosphatase (ALP), (b) – osteocalcin (OCS), (c) – osteopontin (OSP), (d) – collagen I type (COL I). * - $p < 0.05$, $n = 3$. Abbreviations: Ti –smooth titanium surface in medium without osteogenic factors (negative control); Ti + OsteoF – smooth titanium surface in osteogenic medium (positive control); TNT – titania nanotubes in medium without osteogenic factors; TMS – titania mesoporous surface in medium without osteogenic factors; TNT-HA – titania nanotubes with hydroxyapatite in medium without osteogenic factors; TMS-HA – titania mesoporous surface with hydroxyapatite in medium without osteogenic factors.

There is no difference in MTT-assay absorbance after 24 h of cultivation. However, in 5 days the hMSCs cultured on the TNT and TNT-HA have grown faster than on the TMS and TMS-HA, respectively. Although MTT-assay absorbance looks almost at the same level, there is a

statistically significant difference between TMS-HA and TNT-HA compared to TMS and TNT, respectively (Fig S3).

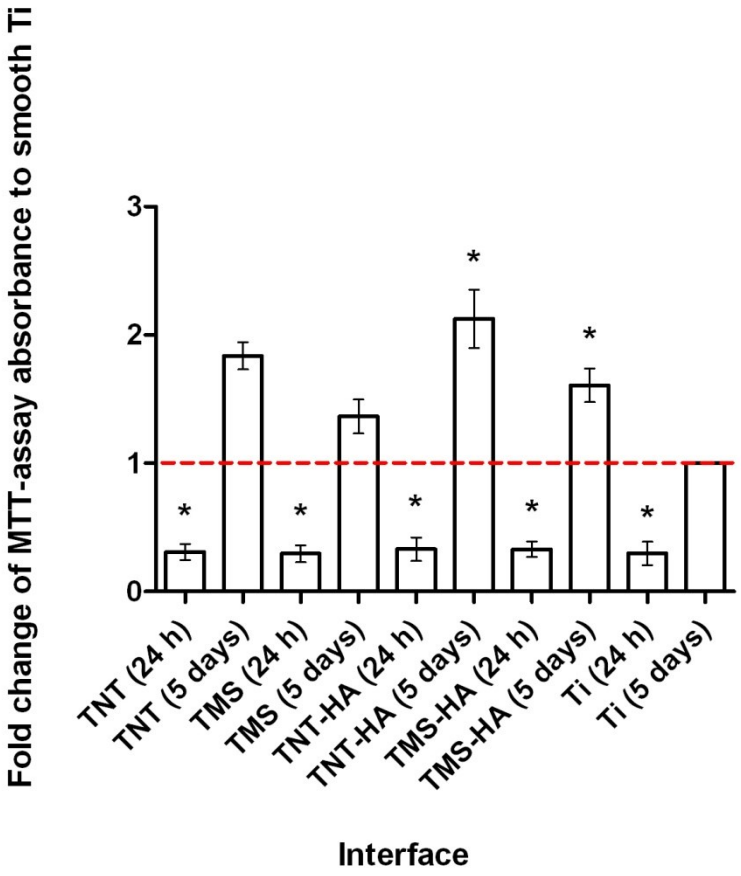

Fig.S3. MTT-assay absorbance of formazan formed by mesenchymal stem cells on titanium (Ti), titania nanotubes (TNT), titania mesoporous surface (TMS), titania nanotubes with hydroxyapatite (TNT-HA), titania mesoporous surface with hydroxyapatite (TMS-HA) after 24 hours and 5 days of incubation. *- $p < 0.05$, $n = 4$.

We highlight that the highly ordered surface morphology (TNT, TNT-HA) is preferable for proliferation, whereas the disordered morphology (TMS and HA-TMS) is better for the osteogenic differentiation of the hMSCs. But in which point is a functional state of hMSCs shifted from the proliferation to the osteogenic differentiation?

C-MYC is a pivotal regulator of cellular growth and proliferation. The up-regulation of C-MYC enhances cellular self-renewal and proliferation, inhibits cellular differentiation, and contracts the focal adhesion of cells. On the contrary, the down-regulation of C-MYC leads to the inhibition of cellular self-renewal and proliferation, the stimulation of cellular differentiation, and the enlargement of focal adhesion of cells[17]. C-MYC has been characterized as a marker gene for mesenchymal stem cell and osteoblast growth[18]. Fig. S4 reflects the gene expression of C-MYC inside hMSCs on the ordered and disordered interfaces at different time points. The up-regulation of C-MYC enhances cellular self-renewal and proliferation, inhibits cellular differentiation, and contracts the focal adhesion of cells. On the contrary, the down-regulation of C-MYC leads to the inhibition of cellular self-renewal and proliferation, the stimulation of cellular differentiation, and the enlargement of focal adhesion of cells[17]. In 3 day, Fig. S4 shows the increase of C-MYC expression inside the hMSCs cultured on the disordered TMS and TMS-HA compared to hMSCs grown on the smooth Ti. Based on the data, the proliferation of hMSCs on the disordered TMS and TMS-HA can be stimulated for 5 days, and then it can be inhibited. A sustained increase of C-MYC expression inside hMSCs in 5 days is observed on the ordered TNT and TNT-HA. Such dynamics of C-MYC

gene expression can point at the proliferation of hMSCs on the ordered TNT and TNT-HA by 5-th day.

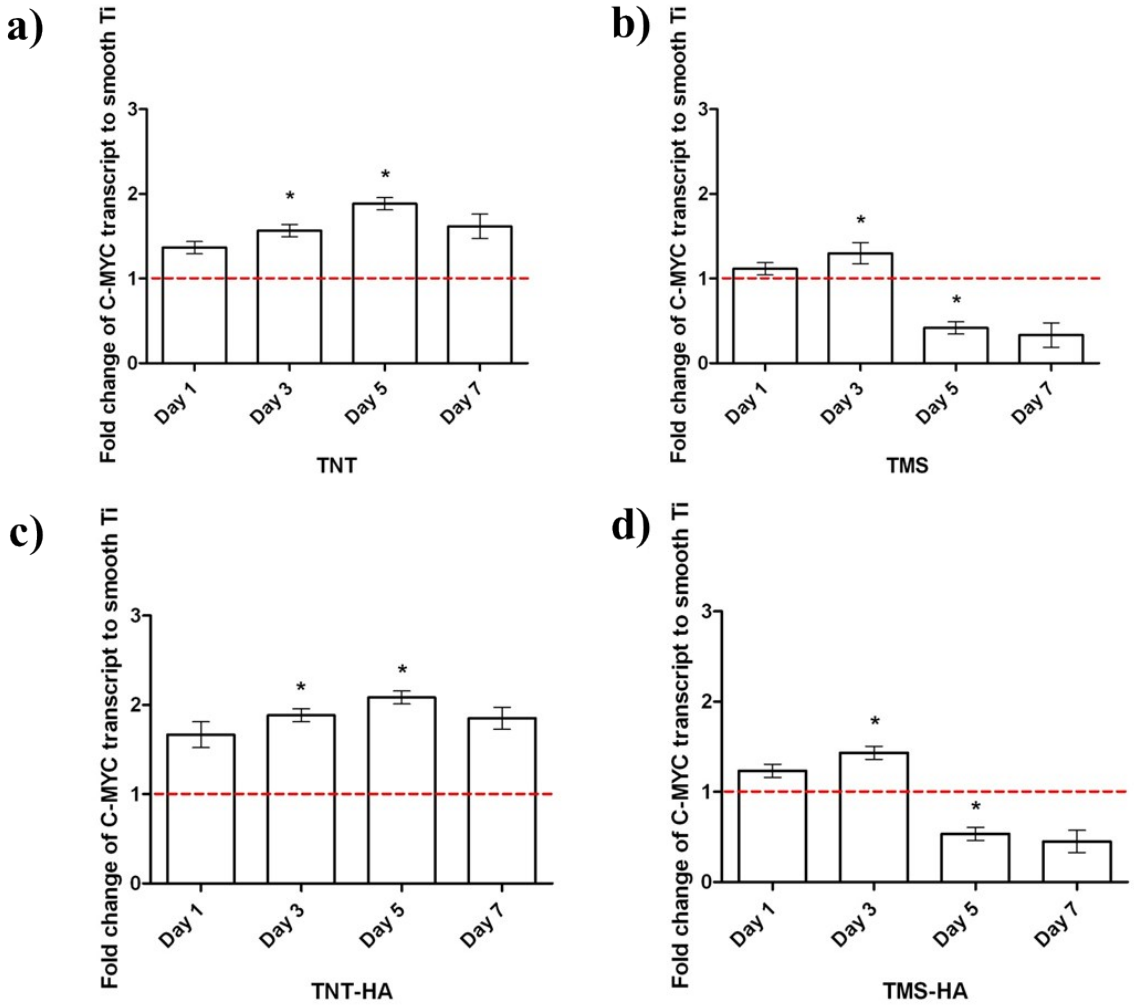

Fig. S4. Dynamics of C-MYC gene expression in mesenchymal stem cells on titania nanotubes (TNT) (a), titania mesoporous surface (TMS) (b), titania nanotubes with hydroxyapatite (TNT-HA) (c), titania mesoporous surface with hydroxyapatite (TMS-HA) (d). * - $p < 0.05$, $n = 3$.

RUNX 2 is another principal transcription factor for the osteogenic differentiation of stem cells. RUNX 2 plays the regulatory role in passage from the self-renewal to the osteogenic differentiation of stem cells[19-22]. The gene expression of RUNX2 inside hMSCs on the ordered and disordered interfaces at different time points is detailed in Fig. S5. The same transcript level of RUNX2 inside hMSCs on the ordered TNT and TNT-HA and polished smooth Ti shows the absence of stem-cell differentiation into the osteogenic direction. Compared to the smooth Ti, the gene expression of RUNX2 inside hMSCs on the disordered TMS and TMS-HA is changed in a wave manner from 1 to 14 days. And there is a significant increase of RUNX-2 on 5-th and 7-th days. Thus, on 5-th day there is C-MYC gene expression decrease accompained by increase of RUNX2 in cells cultivated on the disordered TMS and TMS-HA. As a result, the osteogenic differentiation of hMSCs can be triggered. The transitional point between the proliferation and osteogenic differentiation of hMSCs is 5-th day. However, the up-regulation of RUNX-2 is not stable and is gradually fallen to its transcript level, which is inside hMSCs on the smooth Ti. The alteration of RUNX 2 gene expression in a temporally wave manner indicates that the impact of RUNX2 on the osteogenic transcription regulation depends on the stage of stem-cell differentiation into the osteogenic direction. The up-regulation of RUNX2 at the early stage of osteogenic differentiation is connected to the increased expression of bone-tissue genes, in particular osteocalcin, alkaline phosphatase, osteopontin, collagen I type, inside hMSCs on the disordered TMS and TMS-HA at

day 14 (Fig. S2). On the other hand, the down-regulation of RUNX2 is coincided with the absence of bone-tissue gene induction inside hMSCs by ordered TNT and TNT-HA at 14-th day (Fig. S2).

The MTT-assay data (Fig. 4, ESI Fig. S3) correspond to the C-MYC gene (ESI, Fig. S4) and RUNX2 (ESI, Fig. S5) analysis. Based on these data, we can conclude that the proliferation of hMSCs is higher on ordered TNT and TNT-HA than on the disordered TMS and TMS-HA. It could be explained by different cell behaviour on these samples. For example, the hMSCs only proliferate on the ordered TNT and TNT-HA. Whereas the hMSCs on the disordered TMS and TMS-HA not only proliferate till 5-th day but also differentiate into the osteogenic direction after 5 days. The presence of the raised C-MYC gene expression inside hMSCs on all the mesoporous interfaces (ESI, Fig. S4) corresponds with the fact of the hMSC division process.

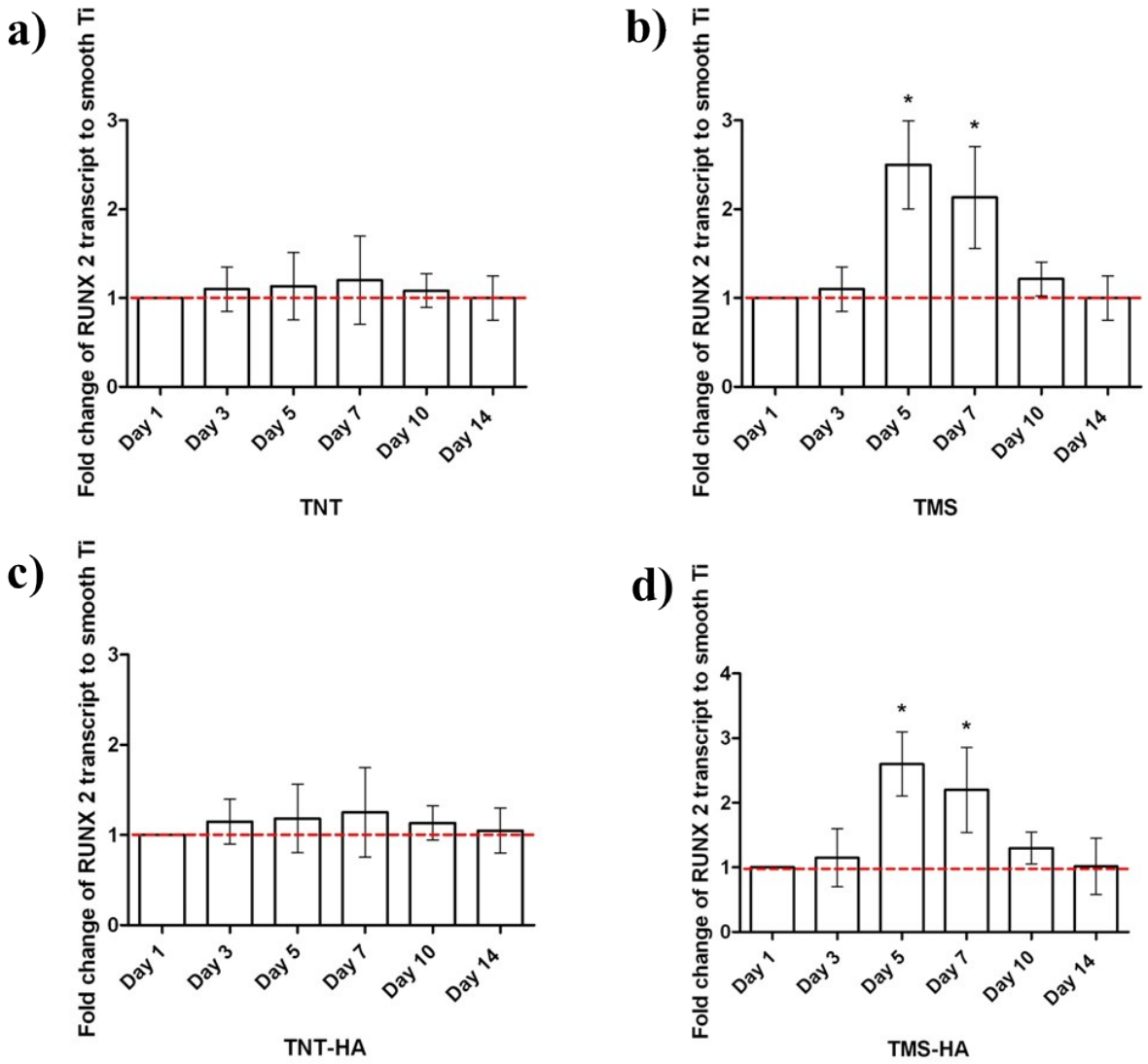

Fig. S5. Dynamics of RUNX 2 gene expression in mesenchymal stem cells on titania nanotubes (TNT) (a), titania mesoporous surface (TMS) (b), titania nanotubes with hydroxyapatite (TNT-HA) (c), titania mesoporous surface with hydroxyapatite (TMS-HA) (d). * - $p < 0.05$, $n = 3$.

Mechanotransduction clarifies how cells process mechanical information of a shape alteration into the response. The osteogenic differentiation of stem cells is accompanied with turning the spindle-like cytoskeletal shape of hMSCs into the star-like cytoskeletal shape of osteoblasts. Consequently, the change of stem-cell cytoskeletal shape on these interfaces in the absence of osteogenic inductors can indicate mechanotransduction processes. Changes in matrix morphology trigger alterations in the tension of the cytoskeleton components in such a way that mechanical forces can be propagated from focal adhesion to the nuclei directly resulting in a transformation of the nucleus shape, chromosomal arrangement, and genes expression involved

in stem-cell self-renewal and differentiation. Moreover, the changes in focal adhesion, caused by a matrix surface morphology stimulus, impact biochemical signaling, that mediates the transcript-factor regulation of gene expression. The more amount of integrins between a cell and a substrate is, the stronger the focal adhesion is.

The Focal adhesion kinase (FAK), also known as protein tyrosine kinase 2 (PTK2), is encoded by the PTK 2 gene. FAK localizes to focal adhesion and regulates signaling in focal adhesion. The principal components of the focal adhesion are integrins, which are αβ heterodimers, regulating the cell-matrix interaction[23]. In addition, the density of hMSCs influences their differentiation through N-cadherins which regulate the cell-cell interaction[24, 25].

Mitogen-activated protein kinases (MAPKs) is offered to be a switcher to guide alterations in the self-renewal and differentiation of mesenchymal stem cells. Descending cellular adhesion signalling is the MAPK extracellular signal-related kinase1/2 (ERK1 (MAPK3)/ERK2 (MAPK1)) that are a crucial controller of self-renewal and are likewise investigated for their function in phosphorylation of transcription factors regulating stem-cell differentiation[26,27]. Fig. S6 highlights the RT-qPCR analysis of regulatory transcription genes, which are PTK2, ERK1/2, after 5-day incubation of hMSCs on the Ti, TNT, TNT-HA, TMS, TMS-HA.

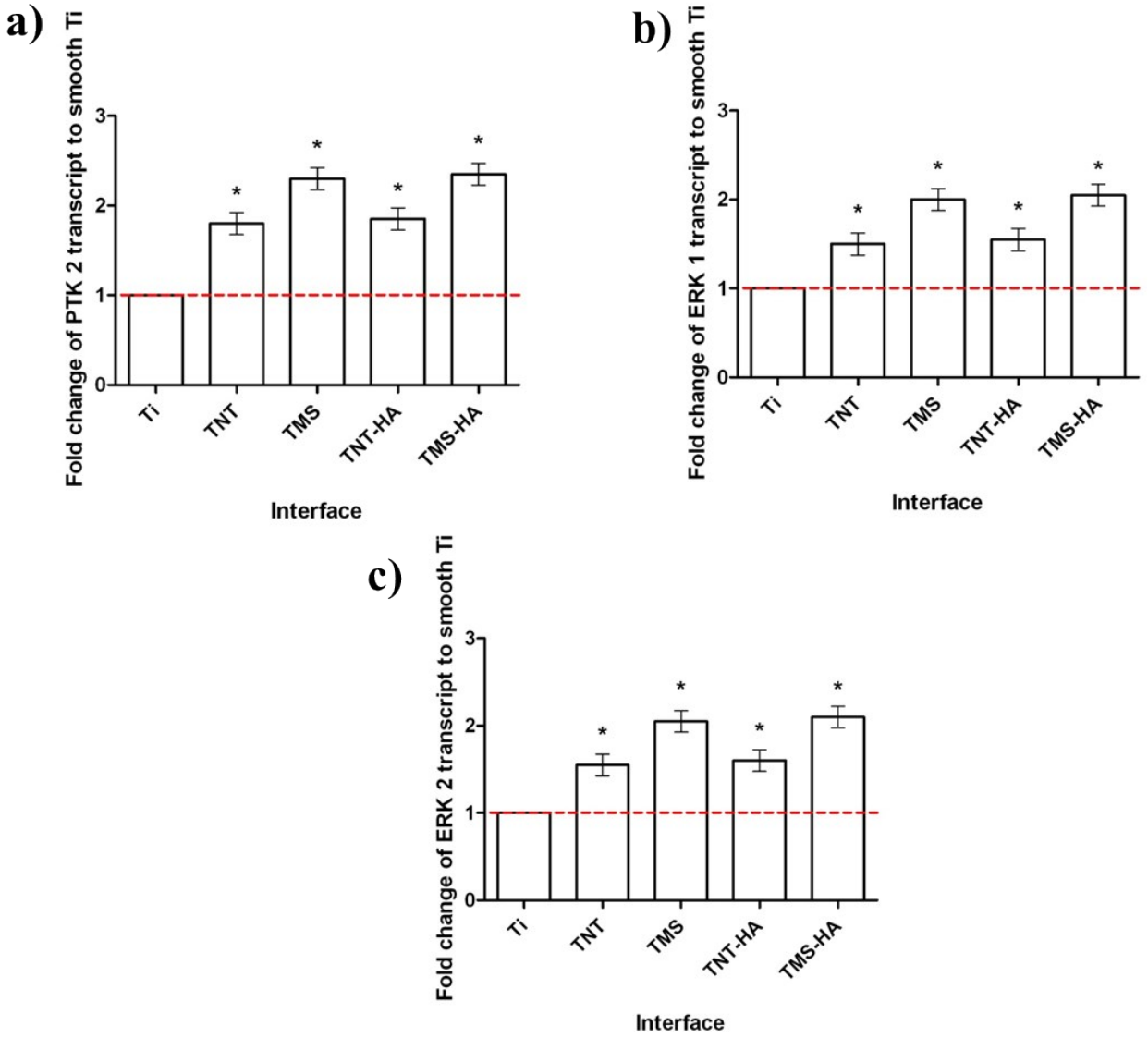

Fig. S6. Expression of regulatory transcription genes after 5-day incubation of mesenchymal stem cells on interfaces. (a) – protein tyrosine kinase 2 (PTK2), (b) – extracellular signal-regulated kinase 1 (ERK1), (c) – extracellular signal-regulated kinase 2 (ERK2). * - $p < 0.05$, $n = 3$. Abbreviations: Ti – smooth titanium surfaces; TNT – titania nanotubes; TMS – titania mesoporous surface; TNT-HA – titania nanotubes with hydroxyapatite; TMS-HA – titania mesoporous surface with hydroxyapatite.

Fig. S7 details the gene expression of cyclin D1 and CDK6 in hMSCs on the ordered morphology of the implant interfaces. Due to the low cytoskeletal tension, cytoplasmic-nuclear Yes-associated protein (YAP) equilibrium is sustained. Mitogenic switches, notably ERK1/2, can guide the cell cycle to support cellular growth by shifting the cycle to prolonged G1 and reduced G2 phases, henceforth potentially suppressing osteogenic differentiation[24, 28–31]. Along with that, weaker focal adhesion related to the smooth titanium surface gives the less proliferation of hMSCs.

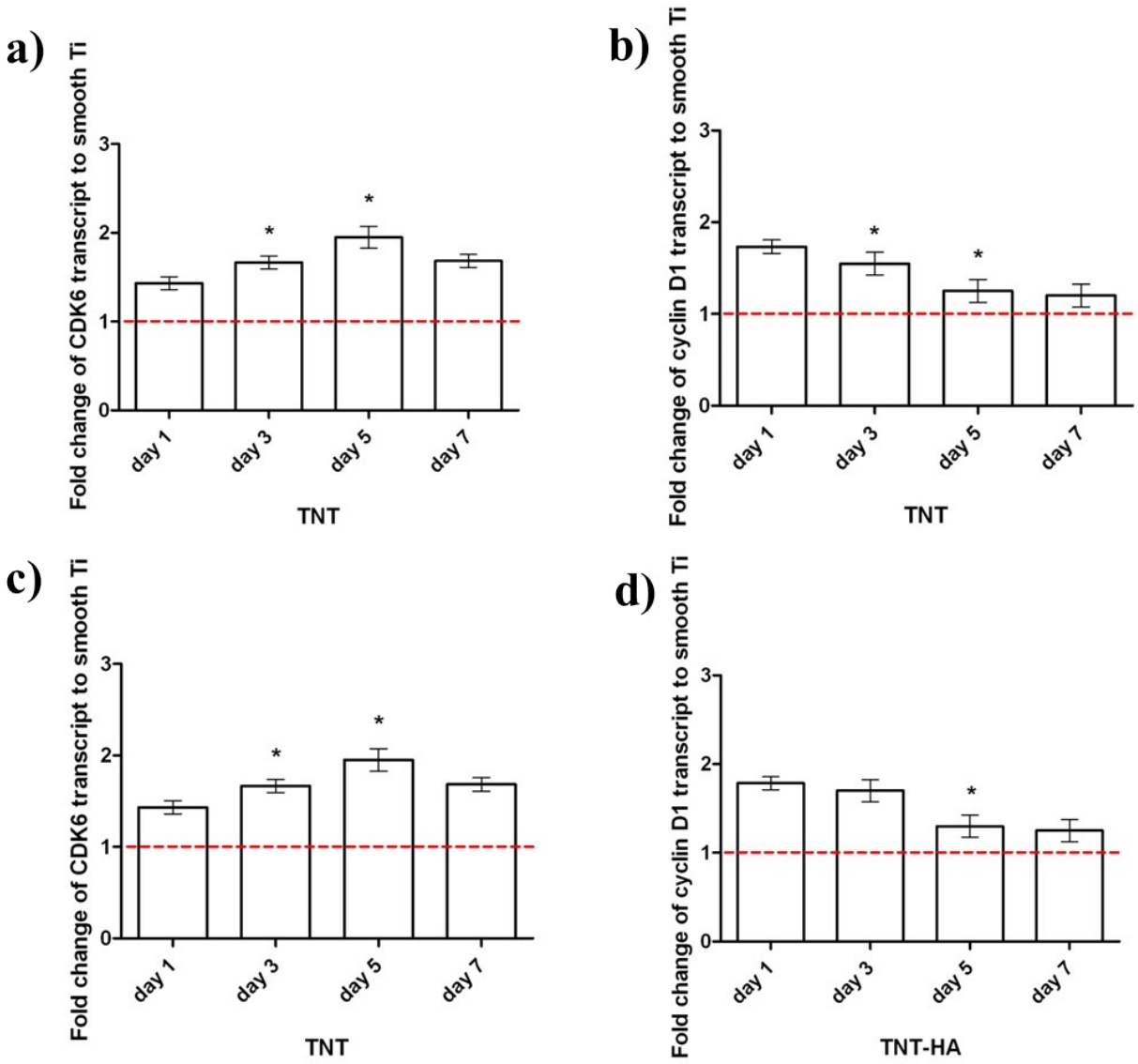

Fig. S7. Gene expression of cyclin-dependent kinase 6 (CDK6) and cyclin D1 in mesenchymal stem cells on ordered titania nanotubes (TNT) (a, b) and titania nanotubes with hydroxyapatite (TNT-HA) (c, d). * - $p < 0.05$, $n = 3$.

The RB phosphorylation takes part in delaying progression to the S phase and triggering RUNX2. The down regulation of the cell-cycle-related transcription factor (E2F1) likewise represses the transition from the G1 to the S phase. Fig. S8 details the gene expression of RB and E2F1 in hMSCs on the disordered morphology of the implant interfaces.

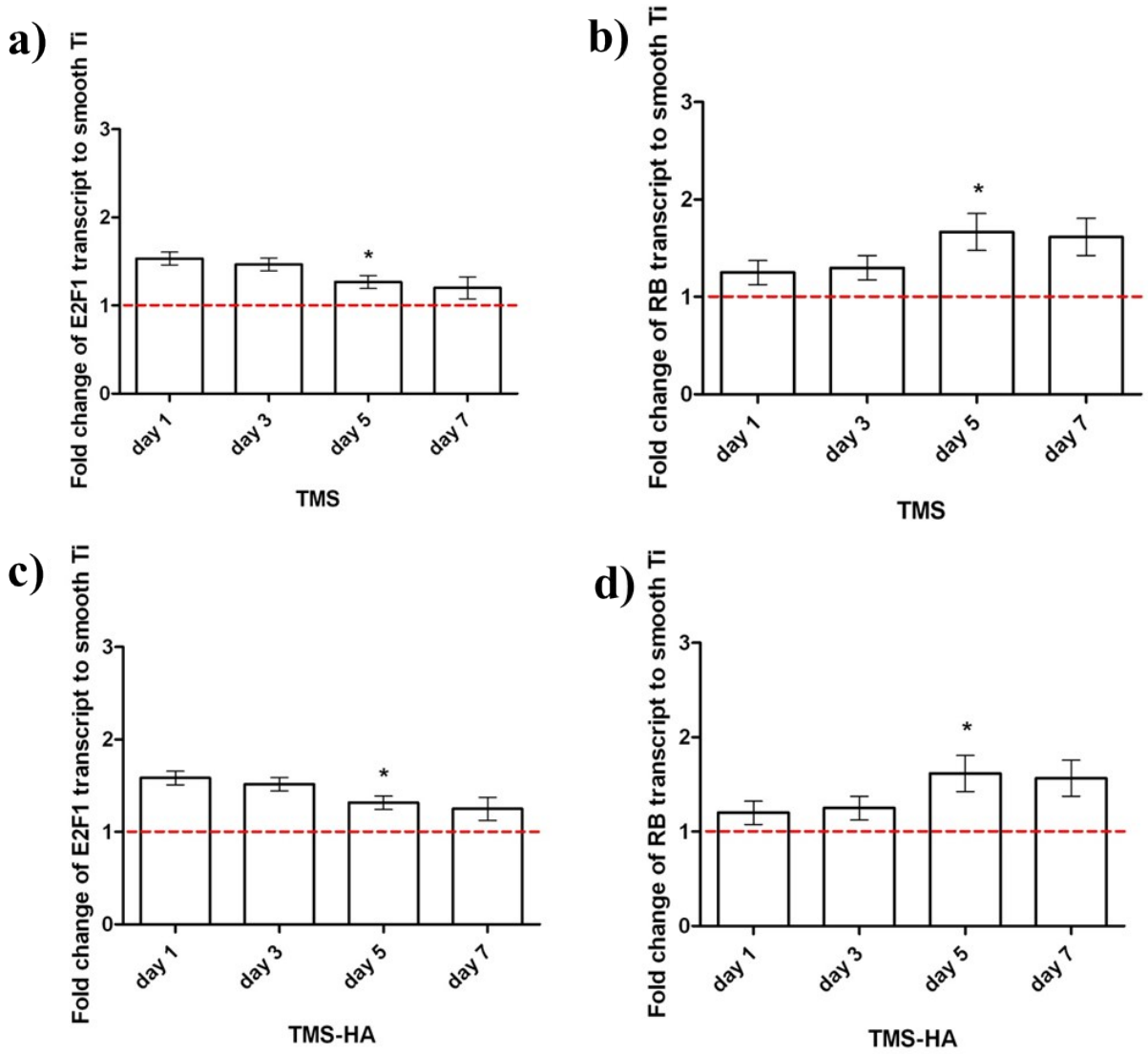

Fig. S8. Gene expression of cell-cycle-related transcription factor (E2F1) and retinoblastoma-associated protein (RB) in mesenchymal stem cells on disordered titania mesoporous surface (TMS) (a, b) and disordered titania mesoporous surface with hydroxyapatite (TMS-HA) (c, d). * - $p < 0.05$, $n = 3$.

Mechanotransduction clarifies how cells process mechanical information of a phenotype alteration into the response. The implant interfaces of interest differ from each other in only their morphology. The osteogenic differentiation of stem cells is accompanied with the change of stem-cell phenotype. In our experiments, we have observed turning the spindle-like cytoskeletal shape of hMSCs into the star-like cytoskeletal shape of osteoblasts on the disordered titania morphology of implant interfaces and fig. S2-S8 has been demonstrated the increased expression of critical osteoblast genes, that are osteocalcin, alkaline phosphatase, osteopontin, collagen type I, during the incubation of hMSCs on these implant interfaces. In another way, the hMSCs maintain the spindle-like cytoskeleton shape on the ordered titania morphology of implant interfaces and Figs. S2-S3 have been reflected hMSCs culture growth which is better on these implant interfaces. In addition, as it is seen in Fig. S2, there is not a difference in the gene expression of osteocalcin, alkaline phosphatase, osteopontin, collagen type I, when hMSCs have been incubated on the ordered titania morphology of implant interfaces. Figs. S4-S8 have been underlined that the expression of regulatory transcription genes, in particular RUNX 2, C-MYC, PTK 2, ERK 1/2, E2F1, RB, CDK6, Cyclin D1, inside hMSCs is distinguished on the ordered and disordered titania morphology of implant interfaces. Consequently, the change of stem-cell phenotype on these interfaces in the absence of the chemical inductors can indicate mechanotransduction processes.

References

1 K. Shimizu, H. Habazaki, P. Skeldon, G.E. Thompson, Radiofrequency GDOES: a powerful technique for depth profiling analysis of thin films. Surface and Interface Analysis: *An International Journal devoted to the development and application of techniques for the analysis of surfaces, interfaces and thin films*, 2003, **35(7)**, 564-574.

2 . M. Mohedano, M. Serdechnova, M. Starykevich, S. Karpushenkov, A. C. Bouali, M. G. S. Ferreira, M. L. Zheludkevich, Active protective PEO coatings on AA2024: Role of voltage on in-situ LDH growth. *Materials & Design*, 2017,**120**, 36-46.

3 R. E. Galindo, R. Gago, D. Duday, C. Palacio, Towards nanometric resolution in multilayer depth profiling: a comparative study of RBS, SIMS, XPS and GDOES. *Analytical and bioanalytical chemistry*, 2010, **396(8),** 2725-2740.

4 T. D. Schmittgen, K. J. Livak, Analyzing real-time PCR data by the comparative C_T method, *Nat. Protoc*., 2008, **3**, 1101.

5 S. Kern, H. Eichler, J. Stoeve, H. Kluter, K. Bieback, Comparative analysis of mesenchymal stem cells from bone marrow, umbilical cord blood, or adipose tissue, *Stem Cells*, 2006, **24**, 1294–1301.

6 M. F. Pittenger, A. M. Mackay, S. C. Beck, R. K. Jaiswal, R. Douglas, J. D. Mosca, M. A. Moorman, D. W. Simonetti, S. Craig, D. R. Marshak, Multilineage potential of adult human mesenchymal stem cells*, Science,* 1999, **284.5411,** 143–147.

7 S. Kern, H. Eichler, J. Stoeve, H. Kluter, K. Bieback, Comparative analysis of mesenchymal stem cells from bone marrow, umbilical cord blood, or adipose tissue, *Stem Cells*, 2006, **24**, 1294–1301.

8 K. Le Blanc, D. Mougiakakos, Multipotent mesenchymal stromal cells and the innate immune system, *Nat. Rev. Immunol.*, 2012, **12.5**, 383–396.

9 A. Aldahmash, M. Haack-Sørensen, M. Al-Nbaheen, L. Harkness, B. M. Abdallah, M. Kassem, Human serum is as efficient as fetal bovine serum in supporting proliferation and differentiation of human multipotent stromal (mesenchymal) stem cells in vitro and in vivo, *Stem Cell Rev. Rep.*, 2011, **7.4**, 860–868.

10 K. Gelse, E. Poschl, T. Aigner, Collagens – structure, functions, and biosynthesis, *Adv. Drug. Deliv. Rev*., 2003, **55.12**, 1531–1546.

11 B. Wildemann, M. Lubberstedt, N. P. Haas, M. Raschke, G. Schmidmaier, IGFI and TGF-beta 1 incorporated in a poly(D,L-lactide) implant coating maintain their activity over long-term storage cell culture studies on primary human osteoblast-like cells. *Biomaterials*, 2004, **25.17**, 3639-3644.

12 H. M. Khandwala, S. Mumm, M. P. Whyte, Low serum alkaline phosphatase activity and pathologic fracture: case report and brief review of hypophosphatasia diagnosed in adulthood, *Endocr. Pract*., 2007, **12.6**, 676–681.

13 H. Orimo, The mechanism of mineralization and the role of alkaline phosphatase in health and disease, *J. Nippon Med. Sch.,* 2010, **77.1**, 4–12.

14 L. Malaval, F. Liu, P. Roche, J. E. Aubin, Kinetics of osteoprogenitor proliferation and osteoblast differentiation in vitro, *J. Cell Biochem.*, 1999, **74**, 616–627.

15 N. K. Lee, Endocrine regulation of energy metabolism by the skeleton, *Cell*, 2007, **130.3**, 456–459

16 F. P. Reinholt, K. Hultenby, A. Oldberg, D. Heinegård, Osteopontin – a possible anchor of osteoclasts to bone, Proc. Natl. Acad. Sci. USA, 2007, **87.12**, 4473–4475.

17 T. Aizawa, S. Kokubun, T. Kawamata, Y. Tanaka, H. I. Roach, c-Myc protein in the rabbit growth plate. Changes in immunolocalisation with age and possible roles from proliferation to apoptosis, *J. Bone Joint Surg. Br.*, 1999, **81.5**, 921925.

18 J. B. Lian, G. S. Stein, Concepts of osteoblast growth and differentiation: basis for modulation of bone cell development and tissue formation. *Crit. Rev. Oral Biol. Med*. 1992, **3.3**, 269305.

19 M. Galindo, J. Pratap, D. W. Young, H. Hovhannisyan, H. J. Im, J. Y. Choi, J. B. Lian, J. L. Stein, G. S. Stein, A. J. van Wijnen, The bone-specific expression of Runx 2 oscillates during the cell cycle to support a G1-related antiproliferative function in osteoblasts, *J. Biol. Chem.*, 2005, **280.21**, 2027420285.

20 J. Pratap, A. Javed, L. R. Languino, A. J. van Wijnen, J. L. Stein, G. S. Stein, J. B. Lian, The Runx 2 osteogenic transcription factor regulates matrix metalloproteinase 9 in bone metastatic cancer cells and controls cell invasion, *Mol. Cell Biol.*, 2005, **25.19**, 85818591.

21 D. M. Thomas, S. A Johnson, N. A Sims, M. K. Trivett, J. L. Slavin, B. P. Rubin, P. Waring, G. A. McArthur, C. R. Walkley, A. J. Holloway, D. Diyagama, J. E. Grim, B. E. Clurman, D. D. L. Bowtell, J.-S. Lee, G. M. Gutierrez, D. M. Piscopo, S. A Carty, P. W. Hinds, Terminal osteoblast differentiation, mediated by Runx 2 and p27KIP1, is disrupted in osteosarcoma, *J. Cell Biol.*, 2004, **167.5**, 925934.

22 J. J. Westendorf, S. K. Zaidi, J. E. Cascino, R. Kahler, A. J. van Wijnen, J. B. Lian, M. Yoshida, G. S. Stein, X. Li, Runx 2 (Cbfa1, AML3) interacts with histone deacetylase 6 and represses the p21(CIP1/WAF1) promoter, *Mol. Cell Biol*., 2002, **22.22**, 79827992.

23 B. Geiger, A. Bershadsky, R. Pankov, K. M. Yamada, Transmembrane extracellular matrix-cytoskeleton crosstalk. *Nat. Rev. Mol. Cell Biol.*, 2001, **2.11**, 793–805.

24 L. Bian, M. Guvendiren, R. L. Mauck, J. A. Burdick, Hydrogels that mimic developmentally relevant matrix and N-cadherin interactions enhance MSC chondrogenesis, *Proc. Natl Acad. Sci. USA*, 2013, **110.25**, 10117-10122.

25 E. V. Kuvyrkov, S. M. Kosmacheva, N. A. Belyasova, Chondrogenic differentiation of human mesenchymal stem cells in 3D fibrin scaffold. *Proceedings of the National Academy of Sciences of Belarus. Medicine series*, 2015, **2**, 38–40 (https://vestimed.belnauka.by/jour/article/view/244/244).

26 C. Ge, G. Xiao, D. Jiang, R. T. Franceschi, Critical role of the extracellular signal–regulated kinase–MAPK pathway in osteoblast differentiation and skeletal development, *J. Cell Biol.*, 2007, **176.5**, 709–718.

27 P. M. Tsimbouri, R. J. McMurray, K. V. Burgess, E. V. Alakpa, P. M. Reynolds, K. Murawski, E. Kingham, R. O. Oreffo, N. Gadegaard, M. J. Dalby, Using morphology and metabolomics to identify biochemical effectors of multipotency, *ACS Nano*, 2012, **6.11**, 10239–10249.

28 J. N. Roberts, J. K. Sahoo, L. E. McNamara, K. V. Burgess, J. Yang, E. V. Alakpa, H. J. Anderson, J. Hay, L. A. Turner, S. J. Yarwood, M. Zelzer R. O. C. Oreffo, R. V. Ulijn, M. J. Dalby, Dynamic surfaces for the study of mesenchymal stem cell growth through adhesion regulation, *ACS Nano*, 2016, **10.7**, 6667–6679.

29 L. C. Lee, N. Gadegaard, M. C. de Andrés, L. A. Turner, K. V. Burgess, S. J. Yarwood, J. Wells, M. Salmeron-Sanchez, D. Meek, R. O. Oreffo, M. J. Dalby, Morphology controls cell cycle changes involved with skeletal stem cell self-renewal and multipotency, *Biomaterials*, 2017, **116**, 10–20.

30 T. Ogasawara, H. Kawaguchi, S. Jinno, K. Hoshi, K. Itaka, T. Takato, K. Nakamura, H. Okayama, Bone morphogenetic protein 2-induced osteoblast differentiation requires Smad-mediated down-regulation of Cdk6, *Mol. Cell. Biol.*, 2004, **24.15**, 6560–6568.

31 E. Laurenti, C. Frelin, S. Xie, R. Ferrari, C. F. Dunant, S. Zandi, A. Neumann, I. Plumb, S. Doulatov, J. Chen, C. April, J. B. Fan, N. Iscove, J. E. Dick, CDK6 levels regulate quiescence exit in human hematopoietic stem cells, *Cell Stem Cell*, 2015, **16.3**, 302–313.